Two-Photon Mode Preparation and Matching Efficiency: Definition, Measurement, and Optimization

Stefania Castelletto, Ivo Pietro Degiovanni, Giampiero Furno, Valentina Schettini, Alan Migdall, and Michael Ware

Abstract—**We investigate the coupling efficiency of parametric downconversion light (PDC) into single and multimode optical fibers as a function of the pump beam diameter, crystal length, and walk-off. We outline two different theoretical models for the preparation and collection of either single-mode or multimode PDC light (defined by, for instance, multimode fibers or apertures). Moreover, we define the mode-matching collection efficiency, important for realizing a single-photon source based on PDC output into a well-defined single mode. We also define a multimode collection efficiency that is useful for single-photon detector calibration applications.**

Index Terms—**Nonlinear media, optical fiber coupling, optical fiber measurement applications, optical propagation in nonlinear media, photon beams.**

I. INTRODUCTION

EARLIEST studies of parametric downconversion (PDC) addressed problems in fundamental physics, while more recent studies target applications such as quantum metrology [1] and quantum information [2], [3]. While both of these areas make use of two-photon light, they are distinct applications that present different requirements for that light. The stringent requirements of these applications are driving researchers to optimize the PDC process. For these efforts to succeed, a clear theoretical framework is needed.

II. THEORY

PDC produces a quantum state of light with a two-photon field description (typically one of the photons is referred to as idler and the other as signal). However, if only one photon of the pair is measured, the source exhibits thermal statistics in each mode, but it emits in many modes. We can, however, introduce a certain degree of coherence. By measuring one of the photons, we prepare the other photon in a specific state. The prepared state will be pure only if we project the first PDC photon (called also the heralding photon) into a single mode. In each of the above PDC applications, we prepare one photon by measuring its twin. Thus, for optimization of the process, it is crucial to

have a proper definition and measurement of the efficiency of that preparation and of the related mode-matching.

We present two different models to define and optimize the two-photon-mode preparation and mode-matching efficiencies. They are distinguished by how the heralding photon is collected. One uses a multimode spatial filter, while the second uses a single-mode fiber. We obtain different dependencies of the efficiency on the pump parameters in these two arrangements. This is particularly important for two specific applications: the calibration of a single-photon detector and the realization of a single-photon on demand source (SPOD) [4], [5]. The generic scheme is shown in Fig. 1.

We consider a two-photon wavefunction, written as [6]

$$|\psi\rangle = \int d^2\rho_1 d^2\rho_2 dt_1 dt_2 \tilde{\Phi}(\rho_1, \rho_2, t_1, t_2)|1_{\rho_2, t_2}\rangle|1_{\rho_1, t_1}\rangle \quad (1)$$

where $\rho_{1,2}$ represents the transverse positions of the two output photons at the time $t_{1,2}$ and $\tilde{\Phi}(\rho_1, \rho_2, t_1, t_2)$ is the biphoton field. The wavefunction is analytic only for first-order approximation of the transverse wavevectors (assuming the pump, signal, and idler have narrow transverse angular distributions we can adopt the paraxial approximation), and is calculated by taking the Fourier transform of the pump angular distribution and the phase-matching function with respect to the pump transverse and the signal k-components. Perfect transverse phase-matching is also assumed. The result derived in [7] is

$$\tilde{\Phi}(\rho_1, \rho_2, t_1, t_2) = N_1 \exp\left[\frac{-i(K_i\theta_i^2 + K_s\theta_s\theta_i)\tau}{D}\right]$$

$$\times \exp\left[\frac{-(\mathcal{N}_p - \mathcal{N}_s)^2\tau^2}{D^2 w_p^2 K_p^2}\right]$$

$$\times \exp\left[\frac{2(\mathcal{N}_p - \mathcal{N}_s)\tau\left(y_1 + \frac{\theta_i\tau}{D}\right)}{D w_p^2 K_p}\right]$$

$$\times \exp\left[-\frac{x_1^2 + \left(y_1 + \frac{\theta_i\tau}{D}\right)^2}{w_p^2}\right]\Pi_{DL}(\tau)$$

$$\times \delta(x_1 - x_2)\delta\left(y_1 - y_2 + \frac{(\theta_i + \theta_s)\tau}{D}\right) \quad (2)$$

where $\tau = t_1 - t_2$ and $\Pi_{DL}(\tau) = 1$ for $0 \le \tau \le DL$ and 0 elsewhere. The subscripts s, i, p indicate the signal, idler, and pump. $\theta_{i,s}$ are the central emission angles (in a small angle non-collinear approximation), and $K_{i,s,p} = n_{i,s,p}(\Omega_{i,s,p}, \phi)\Omega_{i,s,p}/c$ describe the directions of the central intensities of the wavevectors. The terms, $\mathcal{N}_p = \Omega_p/c(dn_p(\Omega_p, \phi))/d\phi|_{\phi_o}$ and $\mathcal{N}_s =$
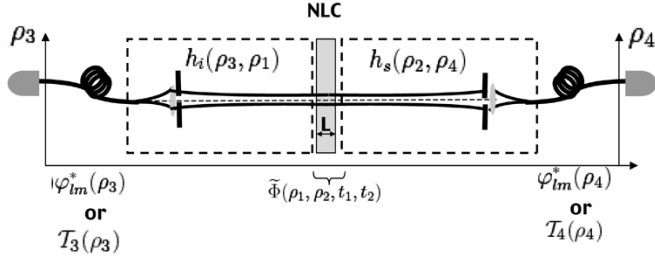
Fig. 1. Unfolded picture of an object corresponding to the idler channel of a PDC source, generated in a nonlinear crystal NLC of length L. The object (on the left) can be either an incoherent or coherent source depending on if the idler beam is prepared by an aperture (or a multimode fiber) or single-mode fiber.

$\Omega_s/c(\mathrm{d}n_s(\Omega_s, \phi))/\mathrm{d}\phi|_{\phi_o}$ account for the effects on the refractive indexes $(n_{p,s,i}(\omega_{p,s,i}, \phi)$ expanded around the central frequencies $(\Omega_{s,i})$, and around the phase-matching angle $\phi_o)$ of the pump and the signal due to the pump angular spread, which are responsible for a small deviation from the phase-matching angle ϕ_o. $D = \mathrm{d}n_s(\omega_s, \phi)\omega_s/c/\mathrm{d}\omega_s|_{\Omega_s} - \mathrm{d}n_i(\omega_i)\omega_i/c/\mathrm{d}\omega_i|_{\Omega_i}$ is the difference of the inverse of the group velocities of the signal and idler, respectively, in the crystal. $D = 0$ s/m and $\mathcal{N}_s = 0$ m^{-1} for type I degenerate phase-matching. The pump-beam transverse field distribution is assumed to be Gaussian with a waist of w_p at the crystal. We also assume that the pump propagates with negligible diffraction inside the crystal.

Envisioning the optics setup as the unfolded scheme of Fig. 1, [8], the source is described by the propagation of a coherent mode defined by $\varphi_{lm}(\rho_3)$ through an optical element with impulse response function $h_i(\rho_3, \rho_1)$, through the nonlinear crystal where the mode gets transformed according to the phase matching function $\tilde{\Phi}(\rho_1, \rho_2, t_1, t_2)$, and collected eventually by $h_s(\rho_2, \rho_4)$. The actual collected mode will then be given by the field $\varphi_{lm}(\rho_4)$. The coincidences measured at the positions 3 and 4 are then $\mathcal{C}_{34}$, the overlap between the PDC fields of both the preparation or collection modes, while the single counts $\mathcal{C}_3$ and $\mathcal{C}_4$ measure the overlap individually between the biphoton field and each of the preparing or collecting modes

$$\mathcal{C}_{34} = \int \mathrm{d}t_1 \mathrm{d}t_2 \left| \int \mathrm{d}^2\rho_1 \mathrm{d}^2\rho_2 \mathrm{d}^2\rho_3 \mathrm{d}^2\rho_4 \tilde{\Phi}(\rho_1, t_1, \rho_2, t_2) \right.$$
$$\left. \times\, h_i(\rho_1, \rho_3) h_s(\rho_2, \rho_4)\varphi_{l'm'}^*(\rho_4)\varphi_{lm}^*(\rho_3) \right|^2$$
$$\mathcal{C}_3 = \int \mathrm{d}t_1 \mathrm{d}t_2 \mathrm{d}^2\rho_4 |\mathrm{d}^2\rho_1 \mathrm{d}^2\rho_2 \mathrm{d}^2\rho_3 \tilde{\Phi}(\rho_1, t_1, \rho_2, t_2)$$
$$\times\, h_i(\rho_1, \rho_3) h_s(\rho_2, \rho_4)\varphi_{lm}^*(\rho_3) |^2$$
$$\mathcal{C}_4 = \int \mathrm{d}t_1 \mathrm{d}t_2 \mathrm{d}^2\rho_3 |\mathrm{d}^2\rho_1 \mathrm{d}^2\rho_2 \mathrm{d}^2\rho_3 \tilde{\Phi}(\rho_1, t_1, \rho_2, t_2)$$
$$\times\, h_i(\rho_1, \rho_3) h_s(\rho_2, \rho_4)\varphi_{lm}^*(\rho_4) |^2. \tag{3}$$

The single-mode matching efficiency is then

$$\chi_M = \frac{\mathcal{C}_{34}}{\sqrt{\mathcal{C}_3 \mathcal{C}_4}} \tag{4}$$

while the single-mode preparation efficiency is

$$\chi_{P(3,4)} = \frac{\mathcal{C}_{34}}{\mathcal{C}_{3,4}}. \tag{5}$$

Specifically, we calculate the efficiency in a perfect imaging configuration, namely $h_s(\rho_2, \rho_4) = \delta(\rho_2 - M_4\rho_4)$ and $h_i(\rho_3, \rho_1) = \delta(\rho_1 - M_3\rho_3)$ (lenses of infinite aperture with magnification M_{j+2}). The lenses are arranged to place the preparation and collection beam waists, $w_{o,j}$ at the crystal, with guided Gaussian field modes

$$\varphi_{10}(\rho_{j+2}) = \sqrt{\frac{2}{\pi}} \frac{M_{j+2}}{w_{o,j}} \exp\left[-\frac{\rho_{j+2}^2 M_{j+2}^2}{w_{o,j}^2} \right]$$

with $j = 1, 2$. The spatial coherence of the single guided modes in the signal and idler arms should ultimately match the overall spatial coherence of the two-photon states.

In the case of the two-photon multimode matching and preparation efficiency, we must calculate the collapse of the PDC wave function over the spatial distribution of multimode fibers or spatial filters (apertures). Assuming again the unfolded scheme of Fig. 1, the source is incoherent with finite transverse distribution $\mathcal{T}_3(\rho_3)$. The collecting modes are then defined by the spatial filter and given by $\mathcal{T}_4(\rho_4)$. The coincidences measured at the positions 3 and 4 are then C_{34}, and C_3 and C_4 are the single counts

$$C_{34} = \int \mathrm{d}t_1 \mathrm{d}t_2 \mathrm{d}^2\rho_3 \mathrm{d}^2\rho_4 \mathcal{T}_4(\rho_4)\mathcal{T}_3(\rho_3)$$
$$\times \left| \int \mathrm{d}^2\rho_1 \mathrm{d}^2\rho_2 \tilde{\Phi}(\rho_1, t_1, \rho_2, t_2) h_i(\rho_1, \rho_3) h_s(\rho_2, \rho_4) \right|^2$$
$$C_3 = \int \mathrm{d}t_1 \mathrm{d}t_2 \mathrm{d}^2\rho_4 \mathrm{d}^2\rho_3 \mathcal{T}_3(\rho_3)$$
$$\times |\mathrm{d}^2\rho_1 \mathrm{d}^2\rho_2 \tilde{\Phi}(\rho_1, t_1, \rho_2, t_2) h_i(\rho_1, \rho_3) h_s(\rho_2, \rho_4)|^2$$
$$C_4 = \int \mathrm{d}t_1 \mathrm{d}t_2 \mathrm{d}^2\rho_3 \mathrm{d}^2\rho_4 \mathcal{T}_4(\rho_4)$$
$$\times |\mathrm{d}^2\rho_1 \mathrm{d}^2\rho_2 \tilde{\Phi}(\rho_1, t_1, \rho_2, t_2) h_i(\rho_1, \rho_3) h_s(\rho_2, \rho_4)|^2. \tag{6}$$

The two-photon multimode matching efficiency is then defined by [9]

$$\eta_M = \frac{C_{34}}{\sqrt{C_3 C_4}} \tag{7}$$

and the two-photon multimode preparation efficiency is defined by

$$\eta_{P(3,4)} = \frac{C_{34}}{C_{3,4}}. \tag{8}$$

We calculate the multimode matching and preparation efficiencies, assuming the incoherent source is completely determined by the functions $\mathcal{T}_{j+2}(\rho_{j+2}) = e^{-(2\rho_{j+2}^2 M_{j+2}^2)/(w_{o,j}^2)}$ which effectively acts as a spatial filter with Gaussian profile, and where the impulse response function is the Dirac delta as before.

In the multimode approach presented here, the preparation and collection modes can be thought of as spatially filtering or selecting the multimode input light. As Fig. 2 demonstrates, the predictions made by this model yield different results than the single-mode model. The multimode model predicts that, for a fixed pump waist, the maximum mode-matching
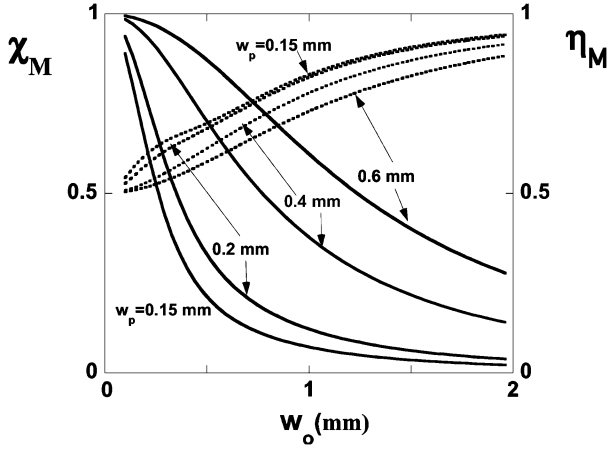
Fig. 2. Plots of η_M (dashed line) and χ_M (solid line) for $w_{o,1} = w_{o,2} = w_o$ and various pump waists, $w_p = 0.15, 0.2, 0.4, 0.6$ mm, versus w_o.

efficiency is obtained when the fiber-defined collection mode (at the crystal) is large, i.e., all the pumped crystal volume is in a region of unit efficiency of the spatial filter system. With the single-mode model, one of the fibers acts as a source of a single-mode beam that propagates through a spatial filter (in this case the pumped crystal volume) to the other fiber. The maximum mode-matching efficiency is achieved with a large pump waist, with respect to the preparation and collection beam waist at the crystal. If the pump waist is smaller than the fiber-defined collection beam waist, the mode-matching efficiency is reduced but it rises with low w_o the efficiency is maximized, constrained with the practical difficulty of having, and aligning, exactly the same selected modes. Here, the differences between the two models are more evident. In fact, when the collection/preparation waist is much greater than the pump waist, η_M asymptotically goes to 1, while χ_M goes to 0; in the opposite condition ($w_p \gg w_o$), $\eta_M \to (1/2)$ and $\chi_M \to 1$.

When we prepare the source in the unfolded scheme in a single mode while we collect in a multimode, the single counts are C_3 in (3), and the coincidences are

$$C_{34} = \int dt_1 dt_2 d^2\rho_4 \mathcal{T}(\rho_4) \left| \int d^2\rho_1 d^2\rho_2 d^2\rho_3 \right.$$

$$\left. \tilde{\Phi}_{12}(\rho_1, t_1, \rho_2, t_2) h_i(\rho_1, \rho_3) h_s(\rho_2, \rho_4) \varphi_{1m}^*(\rho_3) \right|^2. \quad (9)$$

The single-mode preparation and multimode collection efficiency is

$$\epsilon_P = \frac{C_{34}}{C_3}. \quad (10)$$

We explicitly calculate it with a mode preparation given by a single-mode fiber in a near perfect imaging configuration (lens with infinite aperture and magnification M_3 arranged to place the collection beam waist, $w_{o,1}$ at the crystal), described as a Gaussian field, $\varphi_{10}(\rho_3)$, while collecting in a multimode with a Gaussian aperture $\mathcal{T}_4(\rho_4) = e^{-(2\rho_4^2/w^2)}$. The signal optical system is $h_s(\rho_2, \rho_4) = \exp[-ik(\rho_2 - \rho_4)^2)]$ for free-space propagation with $k = \pi/(\lambda_s d)$, and d is the propagation distance.
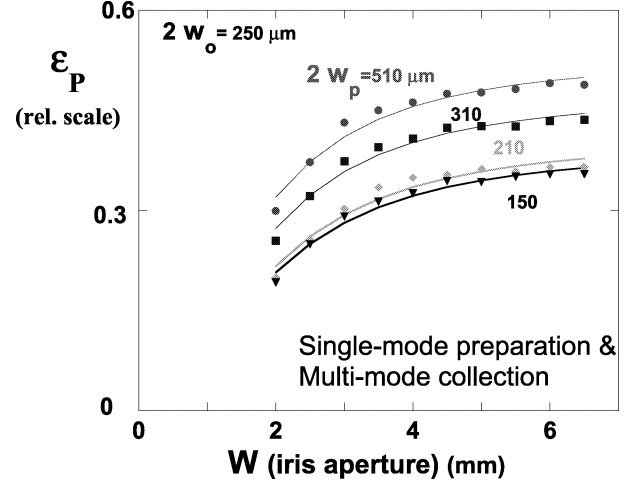
(a)
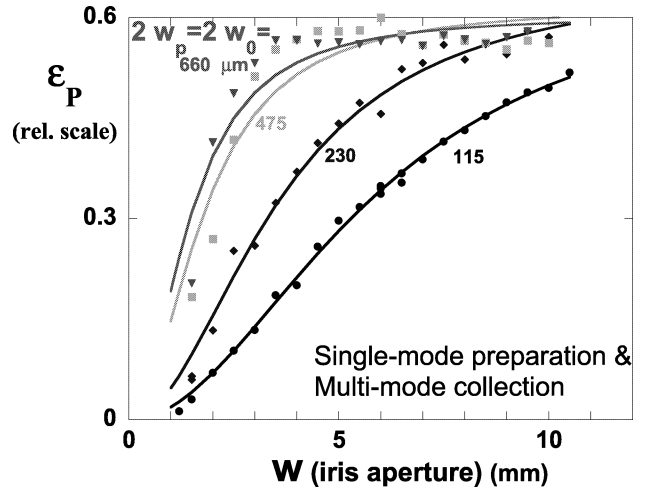
(b)

Fig. 3. Plots of relative ϵ_P data versus the iris diameter w for (a) fixed $2w_o = 250\ \mu$m and (b) $w_p = w_o$, for a range of pump waists as indicated. (a) Measurements performed at IEN, where the efficiency is uncorrected, while (b) measurements performed at NIST, corrected for deadtime. The solid lines are fits to the theory in the thin-crystal limit.

III. EXPERIMENTAL RESULTS

We give here some preliminary experimental results along with theoretical predictions, showing promising agreement. The simulations and measurements are done for type I phase-matching with a pump wavelength of 351.1 nm and a LiIO$_3$ crystal length of 5 mm, with pump diameter at the crystal ranging from from 150–600 μm. Measurements are done with the trigger arm (heralding channel) coupled with a single-mode fiber. The lens images the minimum waist at the crystal. The signal arm is either coupled with a single-mode fiber in a perfect imaging configuration or with a multimode-fiber placed in the focus of the coupling lens, where an iris at the lens selects the collecting modes. Other measurements were performed in a similar setup (6 mm LiIO$_3$) at the National Institute of Standards and Technology (NIST) with the trigger beam coupled with a single-mode fiber and the signal coupled to the detector by a single lens, with an iris selecting the modes. In particular, two experimental configurations were chosen. In one configuration, the trigger mode was fixed to maximize
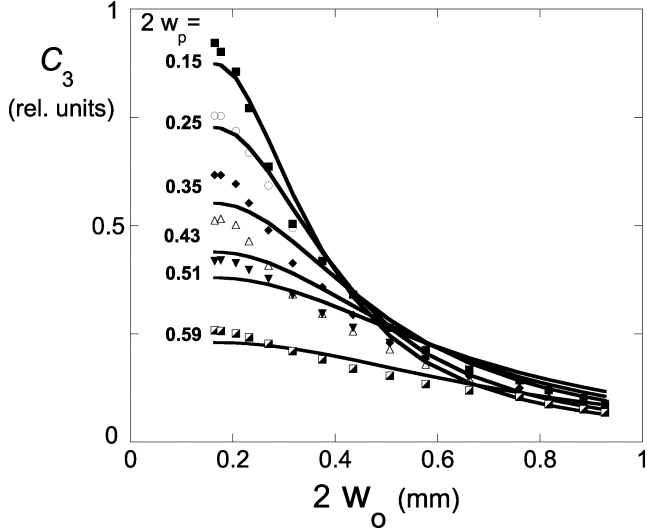
Fig. 4. Plots of single counts $\mathcal{C}_3$ versus w_o for a range of pump waists (millimeters). The maximum counts are for the smallest pump waist.

the singles rate, while in the other configuration the heralding channel waist was matched to the pump waist at the crystal.

In Fig. 3, we show the experimental values of the multimode collection and single-mode preparation efficiency (ϵ_P) versus the collecting iris diameter (w), for the two experimental configurations, i.e., $w_o = w_p$ (a) and $w_o = 250\,\mu m$ (b), for different pump waists. In both cases the maximum efficiency is obtained for larger pump waists as predicted by the theory in Fig. 2. The data are fit to the theoretical model given in the thin crystal limit

$$\epsilon_P = \frac{k^2 w^2 w_o^2 w_p^2 \left(w_o^2 + w_p^2\right)}{\left(w_o^2 + w_p^2\right)^2 + k^2 w_o^2 w_p^2 \left(w^2 w_p^2 + w_o^2 w^2 + w_o^2 w_p^2\right)}.$$

Here we fixed w_o and w_p, while allowing k to vary. We point out that the theoretical prediction of the multimode collection and multimode preparation efficiency (η_P) versus the equivalent Gaussian filter collection aperture $w_{o,2}$ would instead give the maximum efficiency for smaller pump waists. However, while the single-mode preparation and matching efficiency ($\chi_{M,P}$) versus the collecting waist $w_{o,2}$ present a maximum for properly matching the three modes, $\eta_{P,M}$ may not reach the highest efficiency even in this case. Fig. 4 shows the experimental single counts from a heralding channel coupled with a single-mode fiber versus the fiber waist at the crystal, for

various pump waists. Data are fit to theoretical curves that for single-mode coupling are

$$\mathcal{C}_3 = \frac{\mathrm{Erf}\left[\frac{Lq}{\left(\sqrt{w_o^2 + w_p^2}\right)}\right]}{\left(Lq\sqrt{w_o^2 + w_p^2}\right)}$$

where $q = (L\sqrt{2}(-N_p + N_s + K_p\theta_i)/K_p)$. The fit was done by fixing the pump waist and adjusting q. The data match well the single-mode propagation model because we found an optimum preparation waist that maximizes singles rate and the singles rate maximizes for a smaller pump waist. So far, our goal was to show the main difference between multimode and single-mode coupling, where in the multimode coupling the single rates increase with the iris or filter aperture size.

IV. CONCLUSION

In summary, we have presented an analytic model to quantify the mode preparation and matching efficiency in terms of adjustable experimental parameters with the goal of optimizing single-mode collection from PDC sources. In addition, we have presented an alternative scheme that may have more validity for multimode collection arrangements. We reported preliminary experimental results, supporting the validity of the proposed multimode collection configuration.

REFERENCES

[1] A. L. Migdall, S. Castelletto, I. P. Degiovanni, and M. L. Rastello, "Intercomparision of a correlated-photon-based method to measure detector quantum efficiency," *Appl. Opt.*, vol. 41, pp. 2914–2922, 2002.
[2] W. Tittel, J. Brendel, H. Zbinden, and N. Gisin, "Quantum cryptography using entangled photons in energy-time Bell states," *Phys. Rev. Lett.*, vol. 84, pp. 4737–4740, 2000.
[3] E. Knill, R. Laflamme, and G. J. Milburn, "A scheme for efficient quantum computation with linear optics," *Nature*, vol. 409, pp. 46–52, 2001.
[4] T. B. Pittman, B. C. Jacobs, and J. D. Franson, "Single photons on pseudodemand from stored parametric down-conversion," *Phys. Rev. A*, vol. 66, pp. 042 303/1–042 303/7, 2002.
[5] A. Migdall, D. Branning, and S. Castelletto, "Tailoring single-photon and multiphoton probabilities of a single-photon on-demand source," *Phys. Rev. A*, vol. 66, pp. 053 805/1–053 805/4, 2002.
[6] M. H. Rubin, "Transverse correlation in optical spontaneous parametric down-conversion," *Phys. Rev. A*, vol. 54, pp. 5349–5360, 1996.
[7] S. Castelletto, I. P. Degiovanni, A. L. Migdall, and M. Ware, "On the measurement of two-photon single-mode coupling efficiency in parametric down-conversion photon sources," *New J. Phys.*, vol. 6, pp. 87/1–87/16, 2004.
[8] D. N. Klyskho, "Combine EPR and two-slit experiments: Interference of advanced waves," *Phys. Lett. A*, vol. 132, pp. 299–304, 1998.
[9] C. H. Monken, P. H. Ribeiro, and S. Padua, " Optimizing the photon pair collection efficiency: A step toward a loophole-free Bell's inequalities experiment," *Phys. Rev. A*, vol. 57, pp. R2267–R2269, 1998.